A theoretical study of the gas-phase chemi-ionization reaction between uranium and oxygen atoms

Jozef Paulovič
Department of Applied Chemistry, School of Engineering, The University of Tokyo, Tokyo 113-8656, Japan

Laura Gagliardi
Dipartimento di Chimica Fisica "F. Accascina" Viale delle Scienze-Parco d'Orleans II, I-90128 Palermo, Italy

John M. Dyke
Department of Chemistry, University of Southampton, Highfield, Southampton SO17 1BJ, United Kingdom

Kimihiko Hirao[a)]
Department of Applied Chemistry, School of Engineering, The University of Tokyo, Tokyo 113-8656, Japan

(Received 19 October 2004; accepted 2 February 2005; published online 12 April 2005)

The U+O chemi-ionization reaction has been investigated by quantum chemical methods. Potential-energy curves have been calculated for several electronic states of UO and UO^+. Comparison with the available spectroscopic and thermodynamic values for these species is reported and a mechanism for the chemi-ionization reaction $U+O \rightarrow UO^+ + e^-$ is proposed. The U+O and Sm+O chemi-ionization reactions are the first two metal-plus-oxidant chemi-ionization reactions to be studied theoretically in this way. © *2005 American Institute of Physics*.
[DOI: 10.1063/1.1879832]

I. INTRODUCTION

A neutral molecule may undergo ionization by photon or electron impact, as occurs in photoelectron spectroscopy or mass spectrometry. Ionization may also occur on collision of two neutral atomic or molecular species at relative collision energies well below the ionization energies of the colliding species. Such processes are called "chemi-ionization" processes. These reactions are important in a number of areas such as in the earth's upper atmosphere, where they are responsible for the production of ions, notably in the absence of solar radiation,[1] in flames, where ion and electron formation via chemi-ionization plays a significant role,[2,3] and in the technology of magnetohydrodynamic plasmas.[4]

These reactions have been found to occur between a number of metals with unfilled *d* or *f* shells and a number of oxidants, and mass spectra of the ions produced and electron energy distributions have been recorded for a number of metal-oxidant reactions.[5] The simplest case of a metal-oxidant chemi-ionization reaction is the reaction of a metal (M) with atomic oxygen (O). The chemi-ionization reaction to produce the metal oxide ion (MO^+) and an electron is exothermic if the dissociation energy of the neutral metal oxide is greater than its adiabatic ionization energy.

Chemielectron spectra have been interpreted in terms of a classical turning point mechanism. This is depicted schematically in Fig. 1 for the simple associative ionization reaction $M+O \rightarrow MO^+ + e^-$. In this mechanism, the reactants M and O, which correlate with the ground state of MO, approach each other until the left-hand turning point of a MO^* curve is reached (see Fig. 1). Autoionization then occurs in accordance with the Franck–Condon principle and the most intense transition will be a vertical transition onto the MO^+ ground-state curve where the overlap of the initial and final vibrational wave functions is largest. This autoionizing transition can occur at any internuclear separation but has highest probability at the classical turning point.

Using this simple model, any experimental $M+O$ chemielectron spectrum can be interpreted in general as follows. In the electron energy distribution, the highest kinetic energy of the electrons emitted would be equal to the exothermicity of the chemi-ionization reaction. In practice, the highest electron kinetic energy measured will be a lower bound of the reaction exothermicity in cases where a signal associated with the maximum electron energy is not seen because of unfavorable Franck–Condon factors. This quantity is termed the high kinetic-energy offset (HKEO) of a chemielectron band. The maximum intensity of a chemielectron band will occur at an energy corresponding to the vertical energy difference between the MO^* curve at the classical turning point and the MO^+ curve. This quantity has been termed the most probable kinetic energy (MPKE). These values are used to characterize the experimental chemielectron bands (see Fig. 1).

One metal-oxidant chemi-ionization reaction that the Southampton group investigated previously was the reaction of uranium with molecular oxygen.[6] An electron energy distribution was recorded between the thermal beams of the reagents, which showed a single broad asymmetric band with

[a)]Author to whom correspondence should be addressed. Electronic mail: hirao@qcl.t.u-tokyo.ac.jp

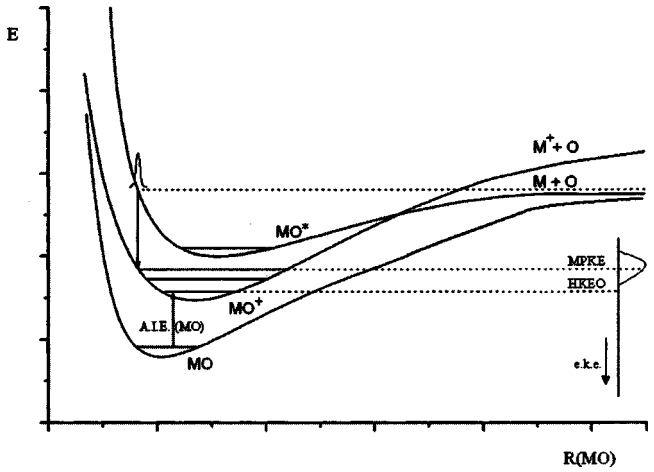

FIG. 1. A schematic potential-energy diagram of $M+O \rightarrow MO^{+}+e^{-}$ chemi-ionization process. MO^{*} is an excited molecular state of MO correlating to the same atomic fragments as MO. In this figure, AIE means adiabatic ionization energy and EKE means electron kinetic energy. HKEO refers to the high kinetic-energy offset and MPKE refers to the most probable electron kinetic energy of a chemielectron band (see text).

a maximum at (0.61 ± 0.08) eV with a tail extending to more than 1 eV beyond the band maximum to high kinetic energies, out to approximately 1.8 eV.

One chemi-ionization channel in the reaction of uranium with molecular oxygen at thermal energies is known, from mass spectrometric studies,[7,8] to be the associative ionization process

$$U + O_2 \rightarrow UO_2^{+} + e^{-}. \tag{1}$$

Although this reaction is responsible for only a small fraction of the overall reaction between uranium and oxygen, the main reaction products being UO and O,[7]

$$U + O_2 \rightarrow UO + O, \tag{2}$$

it nevertheless has a high cross section, $(4.01\pm0.55)\times10^{-17}$ cm^{+2},[8] and has been used as a standard in determining other metal-oxidant chemi-ionization cross sections. However, the chemi-ionization reaction between uranium and oxygen atoms, reaction (3), has an even higher cross section $(3.89\pm0.55)\times10^{-15}$ cm^{+2},[7,8]

$$U + O \rightarrow UO^{+} + e^{-}, \tag{3}$$

and since oxygen atoms are products of the fast neutral reaction (2), reaction (3) must be taken into consideration as a possible source of ions and electrons for the $U+O_2$ reaction under effusive flow conditions. Indeed, kinetic modeling of the uranium plus O_2 system using rate constants derived from measured cross sections for reactions (1)–(3) shows that under the conditions used for the chemielectron experiments,[6] the main source of electrons is reaction (3). The chemielectron spectrum recorded in Ref. 6 was therefore attributed to the U+O chemi-ionization reaction, reaction (3). This reaction would be a very efficient source of ions in the earth's atmosphere if uranium was emitted into the upper atmosphere from, for example, a nuclear accident, and the ions produced could interfere with radio communications.

Although schematic potential-energy curves can be drawn to explain the mechanism of the U+O chemi-ionization,[6] it is only recently that theoretical methods have been developed to compute the reliable potential curves of UO and UO^{+}. In this work we calculate the potential-energy curves of UO and UO^{+} using a method, which includes electron correlation, scalar relativistic effects, and spin–orbit coupling. The objective is to make a comparison of computed and experimental spectroscopic and thermodynamic values for UO and UO^{+} and to propose a mechanism for the observed U+O chemi-ionization reaction, which identifies the states involved. This work follows on from our study on the Sm+O chemi-ionization reaction, which was the first theoretical study of a metal-plus-oxidant chemi-ionization.[9]

The following section presents the Computational Details. The calculated results along with the available experimental values are given in Sec. III. The final section presents the conclusions of the work, along with possible future developments in this area.

II. COMPUTATIONAL DETAILS

In the present study UO and UO^{+} were studied employing the complete active space self-consisted field (CASSCF) method[10] with dynamic electron correlation added via multiconfigurational second-order perturbation theory (CASPT2).[11–14] Scalar relativistic effects were included through the use of the Douglas–Kroll (DK) Hamiltonian.[15,16] The effects of spin–orbit coupling (SOC) were calculated by using the complete active space state interaction (CASSI) method.[17,18] Here, the spin–orbit integrals were computed by the Douglas–Kroll-type of atomic mean-field integral (AFMI) approach.[19] Then the coupling terms were evaluated by allowing the CASSCF wave functions for a range of electronic states to mix under the influence of a spin–orbit Hamiltonian, CASSI-SOC.[20,21] The method has been proven to be successful in the study of other actinide species such as UO_2 (Ref. 22) and U_2.[23] All calculations were performed with the software MOLCAS 6.0.[24]

A newly developed basis set of the atomic natural orbital and relativistic core-correlated (ANO-RCC)-type was used for the two atoms.[25] The exponents were optimized including scalar relativistic effects through the use of the Douglas–Kroll Hamiltonian.[15,16] A primitive set of $27s24p18d14f6g3h$ functions[26] was contracted to $11s10p8d6f3g1h$ for the U atom. For the O atom a primitive set of $14s9p4d3f2g$ basis functions was contracted to $5s4p3d2f$.

In the CASSCF treatment, the [Xe] $4f$, $5d$, $6s$, $6p$ orbitals of U and the $1s$, $2s$ orbitals of O were kept doubly occupied. The active space was formed by ten electrons distributed over 13 active orbitals, i.e., three bonding orbitals which are a linear combination of the O $2p$ orbitals and some U orbitals of appropriate symmetry (of $5f\sigma$, $6d\sigma$, and $6d\pi$), and the corresponding antibonding orbitals, the $7s$ orbital of U, and three bonding U orbitals of $(5f,6d)\pi$, $(5f,6d)\delta$, and $5f\phi$ types, and their corresponding antibonding orbitals. In the subsequent CASPT2 calculations, [Xe] $4f$, $5d$ orbitals of

TABLE I. The spectroscopic constants for the ground state of UO and UO^+. Equilibrium bond length R_e in Angstrom and dissociation energies, D_0 and D_e, in eV. Harmonic vibrational constants ω_e in cm^{-1}. First ionization energy IE (eV) for UO and U atom. In parentheses basis set superposition error corrected values for D_0 and D_e of UO and UO^+ are shown. Previous calculations along with available experimental data are also listed.

System	Method	R_e	D_0	D_e	ω_e	IE
UO						
	RDF-SCF[a]	1.880		−2.050		6.17
	QR-SCMEH-MO[b]			8.790		5.71
	This work					
	spin free	1.850	7.68	7.74	920	6.04
	spin–orbit	1.842	7.52(7.38)	7.57(7.43)	855	6.05
	Expt.[c–e]	1.8383±0.0006	7.86±0.17	7.91±0.17	846.5±0.6	6.0313±0.0006
UO^+						
	AREP-MCSCF-SO[f]	1.842			925	
	This work					
	spin free	1.796	7.78	7.85	1074	
	spin–orbit	1.802	7.66(7.55)	7.72(7.61)	912	
	Expt.[g]		8.02±0.18	[i]		
U	This work					
	spin free					6.09
	spin–orbit					6.20
	Expt.[h]					6.1841±0.0005

[a]Relativistic density functional self-consistent-field calculations (Ref. 31).
[b]Quasirelativistic-self-consistent modified extended Hückel-molecular orbital calculations (Ref. 32).
[c]Reference 28.
[d]Reference 36.
[e]Reference 34.
[f]Averaged relativistic effective potential based multiconfiguration self-consistent-field calculations. The spin–orbit interaction was included through AESOP operator (Ref. 33).
[g]Reference 28.
[h]References 35, 37, and 38.
[i]The experimental D_e of UO^+ cannot be evaluated as $\omega_{e(\text{expt})}$ is not available.

U and 1*s* orbitals of O were kept frozen. All calculations were carried out assuming C_2 symmetry along the internuclear axis, in order to be able to average over the components of degenerate representations (angular momentum larger than zero) in the CASSCF calculations. The potential-energy curves for several electronic states of UO and UO^+ were calculated at the CASPT2 and CASPT2/CASSI-SO levels. The R_e and ω_e spectroscopic constants for the ground states of UO and UO^+ were determined both at the spin-free and spin–orbit levels by using the program VIBROT available in the MOLCAS 6.0 package. The dissociation energy D_e of UO was calculated by subtracting from the total energy of UO at equilibrium $r=R_e$, the energy of the U atom and the O atom calculated separately. A similar procedure was used for UO^+. In the atomic calculations the full diatomic basis set was used in order to correct the basis set superposition error[27] (BSSE). The first ionization energy IE of UO was obtained by subtracting the computed total energies at equilibrium distances for UO and UO^+. The first IE of U was obtained by subtracting from the total energy of the U atom, the total energy of the U^+ ion.

III. RESULTS AND DISCUSSION

The ground states of UO and UO^+ have been experimentally determined as $\Omega=4$ and $\Omega=4.5$, respectively.[28] The computed equilibrium spectroscopic constants, equilibrium bond distance, dissociation energy, and harmonic vibrational constant (R_e, D_e, ω_e) for the ground states for UO and UO^+ are reported in Table I, together with the calculated first ionization energies (IEs) for UO and U atoms. The calculated values of R_e and ω_e for UO are in agreement with the experimental values. For UO^+ there appear to be no experimental values available. For both UO and UO^+, R_e changes very little on including spin–orbit coupling (a decrease of ca. 0.008 Å is computed for UO). According to experiment, $\text{IE(U)} > \text{IE(UO)}$ and $D_0(\text{UO}) < D_0(\text{UO}^+)$. These trends are reproduced by our results. Including spin–orbit coupling, we obtain IE(U)=6.20 eV; IE(UO)=6.05 eV; D_0(UO) =7.52 (7.38) eV; and $D_0(\text{UO}^+)=7.66$ (7.55) eV (BSSE corrected values are in brackets). Table I also presents results of earlier calculations for UO and UO^+.

The ground-state electronic configurations of U, U^+, and O atoms are [Rn] $7s^2 6d^1 5f^3\ ^5L_6$, [Rn] $7s^2 5f^3\ ^4I_{9/2}$, and [He] $2s^2 2p^4$, $^3P_2$, respectively.[29,30] The possible electronic states of UO derived from these states are of the Σ, Π, Δ, Φ, Γ, *H*, *I*, *J*, *K*, *L*, and *M* types. In C_2 symmetry, the Σ, Δ, Γ, *I*, *K*, and *M* states transform into irreducible representation A, while the Π, Φ, *H*, *J*, and *L* states transform into irreducible representation B.

For UO^+ states of Σ, Π, Δ, Φ, Γ, *H*, *I*, *J*, and *K* symmetries are obtained which transform, as shown above in C_2 symmetry. From the above atomic states of U, U^+, and O, the following multiplets have been included in the calculations: triplets, quintets, and septets for UO, and doublets, quartets,

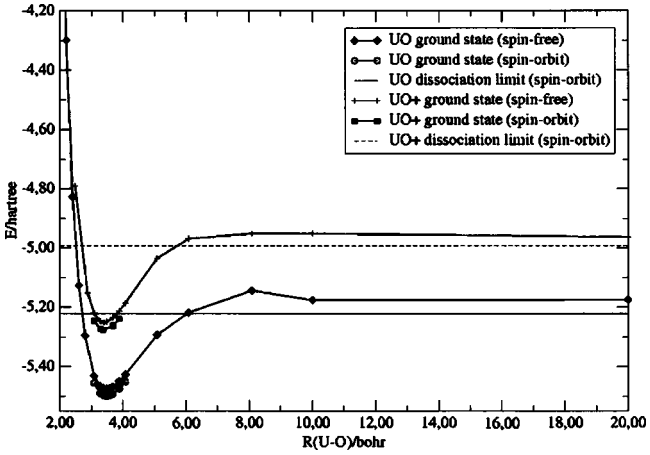

FIG. 2. The spin-free potential-energy curves for the ground-state of UO and the ground-state spin-free potential-energy curve of UO^+. Some points of the spin–orbit potential-energy curves for UO and UO^+ are also shown. The two solid horizontal lines correspond to the calculated spin–orbit energies of neutral atomic reactants in their ground states at dissociation, i.e., U+O and U^++O atoms.

and sextets for UO^+. The potential-energy curves for all these states have been calculated at the CASPT2 and CASPT2/CASSI-SO levels of theory. In Fig. 2, for UO the lowest spin free and part of the lowest spin–orbit curve near equilibrium are shown, together with the lowest spin free and part of the lowest spin–orbit potential-energy curve for the ground state of UO^+. For the calculated triplet, quintet, and septet potential-energy curves for UO we have found that only quintet and septet potential-energy curves were present in the chemi-ionization region. The horizontal line from the U+O dissociation limit encounters septet states of UO first at a bond length of approximately 3.3 bohrs and quintets at a bond length of approximately 3.0 bohrs. The triplet curves all cross this horizontal line at shorter bond lengths. The first UO septet and the first quintet curve encountered by the U+O reagents are shown in Fig. 3. According to our spin-free calculations at the equilibrium bond length, the ground state

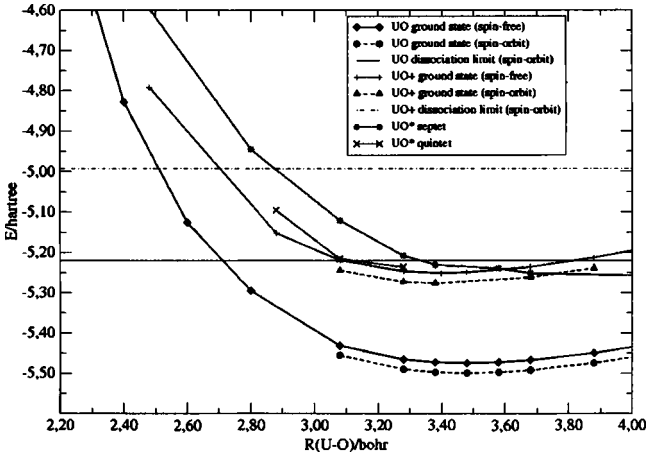

FIG. 3. Enlarged region of the spin-free potential-energy curves for some excited states of UO and the ground state of UO^+, in the U–O bond length region where the chemi-ionization occurs (see text). The two horizontal lines correspond to U+O and U^++O calculated dissociation limits. The first septet and quintet UO^* states which are encountered by the U+O reagents as they approach each other are included in this figure.

of UO arises from $U^{2+}(5f^27s)\ O^{2-}$ and is a doubly degenerate ^5I state. The lowest-lying states arise from $U^{2+}(5f^27s)\ O^{2-}$ and $U^{2+}(5f^27s^2)\ O^{2-}$ configurations. In the first irreducible representation, the following number of roots were considered and taken into account in the spin–orbit calculations: 11 triplets, 24 quintets, and 11 septets. We had to include so many quintet states because we wanted to describe the chemi-ionization region (occurring at ca. 7.7 eV above the ground state). In the second irreducible representation, ten triplets, 24 quintets, and ten septets were considered. The present calculation evaluated 230 spin–orbit states in the first irreducible representation and 220 in the second. From the spin–orbit calculations, the ground state of UO turns out to be a doubly degenerate $^5I_4$ state, which is composed of 71.0% ^5I with small admixtures coming from other components with $\Omega=4$.

According to our spin-free CASPT2 calculations the ground state of UO^+ is a doubly degenerate ^4I state, which can be simply denoted as $U^{3+}(5f^2,{}^4I)O^{2-}({}^1S)$. In the first irreducible representation, the following number of roots were considered and taken into account in the CASPT2/CASSI-SO calculations: six doublets, six quartets, and six sextets, giving 70 spin states in all. From the spin–orbit calculations, the ground state turns out to be the doubly degenerate $^4I_{9/2}$ state, which is composed of 70% ^4I with small admixtures coming from other components with $\Omega=4.5$.

The chemielectron spectrum recorded for the U+O reaction shows a band with a maximum at (0.61 ± 0.08)-eV electron kinetic energy and a tail extending more than 1 eV beyond the band maximum to high electron kinetic energies (up to 1.8 eV). Unfortunately, no vibrational structure was observed in this chemielectron band. Use of the experimental values for D_0 and IE of UO (see Table I) indicates that the chemielectron band should have a maximum kinetic energy of (1.83 ± 0.17) eV (D_0-IE), which compares with 1.47 (1.33) eV derived from the computed spin–orbit values (and 1.64 eV from the computed spin-free values). [The computed spin–orbit value of 1.33 eV has been obtained from the BSSE corrected D_0 for UO and is clearly too low because the computed spin–orbit D_0(UO) is too low by $\approx$0.5 eV, although the computed spin–orbit IE(U) is very good when comparison is made with experimental values.] The experimental high kinetic-energy offset in the chemielectron band is 1.8 eV in good agreement with this experimentally derived (D_0-IE) value of (1.83 ± 0.17) eV. Also, because of poor Franck–Condon factors between the left-hand turning point of the UO^* potential curve and the lowest vibrational levels of the ground state of UO^+, the true high kinetic-energy offset may not have been observed. For the electrons produced in the region of highest chemielectron intensity (at $\approx$0.61 eV), most of the reaction energy is retained in the ion.

An expanded section of Fig. 2 is shown in Figs. 3 and 4. These figures enlarge a region where the horizontal line from the U+O reactants crosses several UO^* states. The reactants U and O correlate with the ground state of UO and several states of UO^*. The reactants approach each other until, in the internuclear distance region from 3.4 to 3.3 bohrs, the horizontal line from the U+O reactants crosses a UO^* curve, which lies above the UO^+ potential curve. This crossing oc-

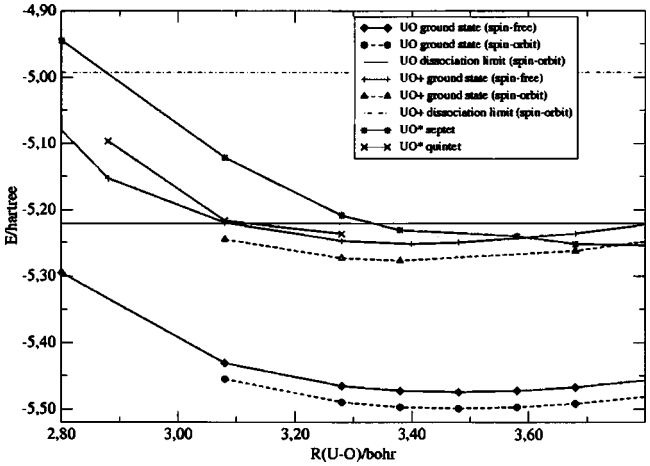

FIG. 4. This is an expanded version of the chemi-ionization region shown in Fig. 3.

curs first with a UO septet state, a $^7\Gamma$ state, at a U–O distance of 3.37 bohrs. On extension of the horizontal line to shorter bond lengths, further septet states are encountered, followed by a group of quintets and a group of triplets states. The first quintet state encountered is a $^5\Delta$ at 3.08-bohr bond length. At the bond length of 3.37 bohrs the UO^* $^7\Gamma$ curve on this line lies 1.50 eV vertically above the UO^+ spin–orbit ground state, a value which is clearly higher than the experimental band maximum of (0.61 ± 0.08) eV. As 3.37 bohrs is close to the computed equilibrium bond length of the ground state of UO^+ of 3.48 bohrs a reasonably sharp chemielectron band would be expected to be centered at 1.50 eV, in poor agreement with the experimental band maximum of (0.61 ± 0.08) eV. Also, it should be borne in mind that the autoionization process $UO^*(^7\Gamma)\rightarrow UO^+(^4I_{9/2})+e^-$ is spin forbidden as ΔS cannot be not zero between the initial and final (ion plus electron) states and therefore this process is likely to be less intense than a spin-allowed process. It can however gain some intensity via spin–orbit coupling and then the selection rule $\Delta\Omega=0$ needs to be satisfied.

A chemielectron band in better agreement with the position and shape of the experimental chemielectron band is expected from the first quintet state encountered, the $^5\Delta$ state. The U+O horizontal line crosses this UO^* state at 3.08 bohrs and at this bond distance, the UO^* state lies 0.65 eV above the UO^+ spin–orbit ground state. Also, the energy separation of the U+O horizontal line from the UO^+ potential-energy minimum is 1.52 eV. Hence a chemielectron band with a maximum at 0.65 eV and a HKEO of 1.52 eV is expected. These values show much better agreement with the experimental MPKE and HKEO values [of (0.61 ± 0.08) and ca. 1.8 eV, respectively].

Also, it should be noted that the autoionization $UO^*(^5\Delta)\rightarrow UO^+(^4I_{9/2})+e^-$ is spin allowed, as the change in S between the initial and final (ion plus electron) states can be zero. The $\Delta\Omega=0$ selection rule can also be satisfied between the $\Omega=4$ in the final state and $\Omega=4$ in the initial $^5\Delta$ state.

The energy levels of UO have been analyzed at a bond distance of 3.08 bohrs, where this chemi-ionization occurs. The $^5\Delta$ state is a split by spin–orbit coupling with a total splitting of its spin–orbit manifold of 3473 cm^{-1}. The energy of the spin-free state up to the highest spin–orbit component ($\Omega=4$, the dominant component in the chemi-ionization process) is 0.21 eV (1718 cm^{-1}).

In summary, the position and shape of the U+O experimental chemielectron band are consistent with chemi-ionization taking place via a UO^* quintet state rather than a UO^* septet state. This $UO^*\rightarrow UO^+ + e^-$ autoionization process satisfies the $\Delta S=0$ and $\Delta\Omega=0$ selection rules. This contrasts with the results obtained for Sm+O (Ref. 9) where comparison of the position and shape of the experimental chemielectron band with that expected from computed potential curves indicated that the chemi-ionization occurs via a mechanism which is spin forbidden ($\Delta S\neq 0$) but spin–orbit allowed ($\Delta\Omega=0$).

IV. CONCLUSIONS

In conclusion, the present study represents the first example of a quantum chemical investigation of an actinide-plus-oxidant chemi-ionization reaction. The potential energy curves for the ground states of UO and UO^+, as well as a number of excited states of UO, have been calculated in order to investigate the mechanism of the U+O chemi-ionization reaction. The UO and UO^+ states involved have been identified and the position of the experimental chemielectron band has been explained on the basis of these potential curves. The comparison between the experimental chemielectron band maximum and band shape with that expected from the calculations indicates that chemi-ionization occurs via the first quintet state of UO encountered in the U+O incoming channel. It is proposed to extend these studies to other metal-plus-oxidant chemi-ionization reactions.

ACKNOWLEDGMENTS

The authors wish to thank Professor Björn Olof Roos for ANO-RCC basis set for U and for valuable advice. This research was supported in part by a Grant-in-Aid for Scientific Research in Specially Promoted Research "Simulations and Dynamics for Real Systems" and Grant for 21st Century COE Program "Human-Friendly Materials based on Chemistry" from the Ministry of Education, Science, Culture, and Sports of Japan, and by a grant from the Genesis Research Institute. One of the authors (J.P.) is grateful for a financial support from the Ministry of Education, Science, Culture, and Sports of Japan. The authors are grateful for excellent computational facilities at the University of Tokyo. One of the authors (J.M.D.) thanks the NERC (UK) for financial support. One of the authors (L.G.) thanks Ministero dell'Istruzione dell'Universita'e della Ricerca (MIUR) for financial support.

[1] T. L. Brown, Chem. Rev. (Washington, D.C.) **73**, 645 (1973).
[2] H. F. Calcote, Combust. Flame **42**, 215 (1981).
[3] A. Fontijn, Prog. React. Kinet. **6**, 75 (1971).
[4] J. Lawton and F. J. Weinberg, *Electrical Aspects of Combustion* (Clarendon, Oxford 1969).
[5] M. C. R. Cockett, J. M. Dyke, A. M. Ellis, M. Feher, and T. G. Wright, J. Electron Spectrosc. Relat. Phenom. **51**, 529 (1990).
[6] J. Baker, M. Barnes, M. C. R. Cockett *et al.*, J. Electron Spectrosc. Relat. Phenom. **51**, 487 (1990).

[7]W. L. Fite, H. H. Lo, and P. Irving, J. Chem. Phys. **60**, 1236 (1974).
[8]J. C. Halle, H. H. Lo, and W. L. Fite, J. Chem. Phys. **73**, 5681 (1980).
[9]J. Paulovič, L. Gagliardi, J. M. Dyke, and K. Hirao, J. Chem. Phys. **120**, 9998 (2004).
[10]B. O. Roos, in *Advances in Chemical Physics: Ab Initio Methods in Quantum Chemistry-II*, edited by K. P. Lawley (Wiley, Chichester, England, 1987), Chap. 69, p. 399.
[11]K. Andersson, P.-Å. Malmqvist, B. O. Roos, A. J. Sadlej, and K. Wolinski, J. Phys. Chem. **94**, 5483 (1990).
[12]K. Andersson, P.-Å. Malmqvist, and B. O. Roos, J. Chem. Phys. **96**, 1218 (1992).
[13]B. O. Roos, K. Andersson, M. P. Fülscher, P.-Å. Malmqvist, L. Serrano-Andrés, K. Pierloot, and M. Merchán, in *Advances in Chemical Physics: New Methods in Computational Quantum Mechanics*, edited by I. Prigogine and S. A. Rice (Wiley, New York, 1996), Vol. XCIII, pp. 219–331.
[14]J. Finley, P.-Å. Malmqvist, B. O. Roos, and L. Serrano-Andrés, Chem. Phys. Lett. **288**, 299 (1998).
[15]M. Douglas and N. M. Kroll, Ann. Phys. (N.Y.) **82**, 89 (1974).
[16]B. A. Hess, Phys. Rev. A **33**, 3742 (1986).
[17]P.-Å. Malmqvist, Int. J. Quantum Chem. **30**, 479 (1986).
[18]P.-Å. Malmqvist and B. O. Roos, Chem. Phys. Lett. **155**, 189 (1989).
[19]B. A. Hess, Ch. M. Marian, U. Wahlgren, and O. Gropen, Chem. Phys. Lett. **251**, 365 (1996).
[20]P.-Å. Malmqvist, B. O. Roos, and B. Schimmelpfennig, Chem. Phys. Lett. **357**, 230 (2002).
[21]B. O. Roos and P.-Å. Malmqvist, Phys. Chem. Chem. Phys. **6**, 2919 (2004).
[22]L. Gagliardi, M. C. Heaven, J. W. Krogh, and B. O. Roos, J. Am. Chem. Soc. **127**, 86 (2005).
[23]L. Gagliardi and B. O. Roos, Nature (London) (in press).
[24]G. Karlström, R. Lindh, P.-Å. Malmqvist *et al.*, Comput. Mater. Sci. **28**, 222 (2003).
[25]B. O. Roos (unpublished).
[26]K. Faegri, Theor. Chem. Acc. **105**, 252 (2001).
[27]S. F. Boys and F. Bernardi, Mol. Phys. **19**, 553 (1970).
[28]L. A. Kaledin, J. E. McCord, and M. C. Heaven, J. Mol. Spectrosc. **164**, 27 (1994).
[29]L. R. Carlson, J. A. Paisner, E. F. Worden, S. A. Johnson, C. A. May, and R. W. Solarz, J. Opt. Soc. Am. **66**, 846 (1976).
[30]D. W. Steinhaus, L. J. Radzienski, and R. D. Cowan, Aeronaut. Space Admin. Spec. Publ. NASA SP-236, 151 (1971).
[31]G. L. Malli, in *The Challenge of d and f Electrons, Theory and Computation*, ACS Symposium Series 394 edited by D. R. Salahub and M. C. Zerner (American Chemical Society, Washington, DC, 1989), Chap. 21, p. 291.
[32]E. A. Boudreaux and E. Baxter, Int. J. Quantum Chem. **90**, 629 (2002).
[33]M. Krauss and W. J. Stevens, Chem. Phys. Lett. **99**, 417 (1983).
[34]J. D. Han, L. A. Kaledin, V. Goncharov, A. V. Komissarov, and M. C. Heaven, J. Am. Chem. Soc. **125**, 7176 (2003).
[35]A. Waldek, N. Erdmann, C. Gruning *et al.*, AIP Conf. Proc. **584**, 219 (2001).
[36]A. Pattoret, J. Drowart, and S. Smoes, *Thermodynamics of Nuclear Materials* (IAEA, Vienna, Austria, 1968), pp. 613–636.
[37]A. Coste, R. Avril, P. Blancard, J. Chatelet, D. Lambert, and J. Legre, J. Opt. Soc. Am. **72**, 103 (1982).
[38]R. W. Solarz, C. A. May, L. R. Carlson, E. F. Worden, S. A. Johnson, J. A. Paisner, and L. J. Radziemski, Phys. Rev. A **14**, 1129 (1976).